

Spectroscopic characterization of bismuth embedded Y zeolites

Hong-Tao Sun,^{1,a)} Yoshio Sakka,² Yuji Miwa,³ Naoto Shirahata,² Minoru Fujii,³ and Hong Gao¹

¹International Center for Young Scientists (ICYS), National Institute for Materials Science (NIMS), 1-2-1 Sengen, Tsukuba-city, Ibaraki 305-0047, Japan

²Nano Ceramics Center, National Institute for Materials Science (NIMS), 1-2-1 Sengen, Tsukuba-city, Ibaraki 305-0047, Japan

³Department of Electrical and Electronic Engineering, Graduate School of Engineering, Kobe University, Rokkodai, Nada, Kobe 657-8501, Japan

(Received 11 August 2010; accepted 12 September 2010; published online 29 September 2010; corrected 5 October 2010)

Bismuth embedded Y zeolites were studied by using UV-vis- near infrared (NIR) diffuse reflectance, Raman, and steady-state NIR photoluminescence spectroscopy. The results suggest that Bi_5^{3+} and Bi^+ active centers coexist in the dehydrated and hydrated zeolite framework, both of which contribute to NIR emission. Furthermore, it was revealed that the high-temperature annealing leads to the formation of Bi_2O_3 clusters, which act as blocks for selectively closing down the “in-out windows” of H_2O and O_2 molecules in the zeolites. It is believed that these materials can find a wide array of applications as active media of broadly tunable micro or nano-optical sources. © 2010 American Institute of Physics. [doi:10.1063/1.3496460]

Zeolite based materials represent a large family of aluminosilicates constituted by corner-linked TO_4 tetrahedra (T stands for either Si or Al) that adopt a remarkable variety of structures containing channels and/or cavities of different dimensions. The zeolite framework has a net negative charge, arising from $[\text{AlO}_{4/2}]^-$ units that replace neutral $[\text{SiO}_{4/2}]$ units, which equals the number of aluminum atoms in the framework.¹⁻¹³ The electrostatic neutrality is ensured by an equivalent number of extraframework cations. This peculiar property, combined with the competitive costs of the zeolite raw materials and adjustable morphological properties of the matrix, makes them great potentials in areas such as catalysis, ion exchange, molecular sieves, or drying agents.¹ Recent results also indicated the potential use of optically functionalized zeolites as luminescent and laser materials.⁴⁻¹³ For instance, Sun *et al.*¹³ demonstrated that Y-type zeolites exchanged with bismuth ions show strong near infrared (NIR) emission after thermally treatment in an inert atmosphere, due to the formation of bismuth related active centers. However, there still exist lots of unsolved scientific difficulties in this area. First, there is not a clear picture on the origin of bismuth active centers, although experimental results suggested that subvalent Bi contributes to the NIR emission. Time-resolved and excitation-wavelength-dependent photoluminescence (PL) results revealed that multitype, rather than single-type bismuth active centers coexist in the Y structure, acting as charge compensators of the framework.^{13,14} One possibility is that Bi^+ is the bismuth related active centers, which locates in different coordination environments in the structure. The other possibility is that more than one type of subvalent Bi centers (i.e., Bi^+ and cationic Bi clusters) cocontribute to the emission. Up till now, it is unclear which scenario is correct. Second, the color of the as-annealed products is green, which becomes shallow pale white after full exposure to air. No results available can reveal what is the reason for this evolution. Third, to explain highly efficient PL from Bi doped zeolites, Sun *et al.*¹³ pro-

posed that there exist Bi related agglomerates in zeolites annealed at high temperatures, which act as blocks for selectively closing down the “in-out windows” of water molecules. However, there is no evidence to support the existence of agglomerates in the samples.

In this letter, to gain a more detailed insight into NIR PL mechanism and Bi distribution in the as-annealed and hydrated Bi embedded zeolites, we characterized the samples by using extensive techniques including UV-vis-NIR diffuse reflectance, Raman, and steady-state NIR PL spectroscopy. The results suggest that Bi_5^{3+} and Bi^+ coexist in the zeolite framework, both of which contribute to NIR emission. Furthermore, the high-temperature annealing leads to the formation of Bi_2O_3 clusters, which act as blocks for selectively closing down the “in-out windows” of H_2O and O_2 molecules in the zeolite framework.

The NH_4 form of Y zeolites were purchased from Tosoh Co. Japan (Zeolite Y, $\text{SiO}_2/\text{Al}_2\text{O}_3=7$). The Bi^{3+} -exchanged zeolites were prepared by a method reported in Ref. 11. The exchanged zeolites were calcined at 750, 830, and 900 °C for 30 min in an Ar atmospheric condition. After thermal treatment, the samples were sealed into glass bottles for further measurements. Note that the samples for treatment at 750 °C were first loaded into glass bottles, then transferred to high temperature region of a tube furnace, and finally quickly sealed by caps when the annealed samples cooled down to room temperature; while for the samples at 830 and 900 °C, the powders were loaded into Al_2O_3 ceramic boats, and quickly transferred and sealed into glass bottles after annealing. Diffuse reflectance spectra of the products were measured by a UV-vis-NIR spectroscope (V-570, JASCO, Japan) equipped with an integrating sphere. To measure the UV-vis-NIR spectra of the as-annealed samples, the powders were quickly transferred into a cell with silica glass window, and then sealed it tightly for measurements. Note that the colors of the samples do not show a notable change after measurements. These samples were denoted as “as-annealed” (also described as “dehydrated”) ones in Figs. 1 and 3 while those exposed to air for 30 min and 24 h were as

^{a)}Electronic mail: timothyhsun@gmail.com.

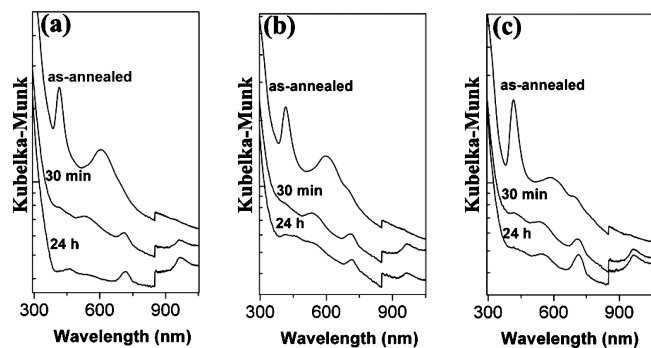


FIG. 1. UV-vis-NIR diffuse reflectance spectra of the samples annealed at (a) 750 °C, (b) 830 °C, and (c) 900 °C. The as-annealed samples are dehydrated ones. 30 min and 24 h are the exposure times of the dehydrated samples in air. Note that for samples exposed to air over 24 h, the color does not show notable change. The steps at 850 nm are due to the measurement artifacts.

“30 min” and “24 h,” respectively. The atomic ratio of Bi/Al in the final products was determined to be $\sim 23\%$ by energy-dispersive x-ray spectroscopy. Raman spectra were performed by using Jobin Yvon T-64 000 system under the excitation of 514.5 nm line from an Ar⁺ laser.

X-ray powder diffraction results revealed that the annealed zeolite structure keeps intact, and no new diffraction peaks except those of zeolite were observed, indicating no new crystalline phases develop in these samples. Interestingly, the as-annealed products show temperature dependence of color development; at 750 °C, the powders are green while at higher temperatures, the samples become shallow green. Figure 1 shows the effect of atmosphere on the absorption property of the samples annealed at different temperature. The as-annealed samples display two main absorption bands centered at 415 and 600 nm and a weak absorption tail over 850 nm; for those annealed at 830 and 900 °C, a new shoulder at ~ 700 nm appears. Exposure the as-annealed samples to air results in a fast color change from green to shallow pale white. The hydrated powers demonstrate absorption bands at 535, 715, and 970 nm in addition to a weak one < 500 nm. The analysis of atmosphere dependence of bismuth active centers leads us to conclude that bismuth active centers occupy at least two kinds of sites in the framework as follows: one kind of site is water and oxygen reachable, where the bismuth active centers can be destroyed by them and the other is separated from them.

Obviously, the absorption bands shown in Fig. 1 cannot be assigned to the electronic transitions of single-type Bi active center, such as Bi³⁺ or Bi²⁺.^{15,16} As is known, bismuth has profound propensity to form clusters or to exist as Bi⁺ in ionic liquids or crystals, which demonstrate strong visible and NIR absorption bands.^{17,18} For instance, Bi₅³⁺ and Bi⁺ can coexist in Bi–GaCl₃–benzene system at various temperatures;¹⁸ the Bi₅³⁺ displays main absorption bands at 428, 520 and 875 nm while Bi⁺ at 609 and 694 nm. It is noteworthy that the absorption characteristics of the as-annealed samples are similar with those of liquids containing Bi₅³⁺ and Bi⁺.¹⁸ This leads us to postulate that Bi₅³⁺ and Bi⁺ coexist in our as-annealed zeolites; that is, Bi₅³⁺ is the 415 nm related bismuth active centers, and Bi⁺ results in strong absorption centered at 600 nm. Once the sample is hydrated, Bi₅³⁺ or Bi⁺ ions at water/oxygen-reachable sites are destroyed.

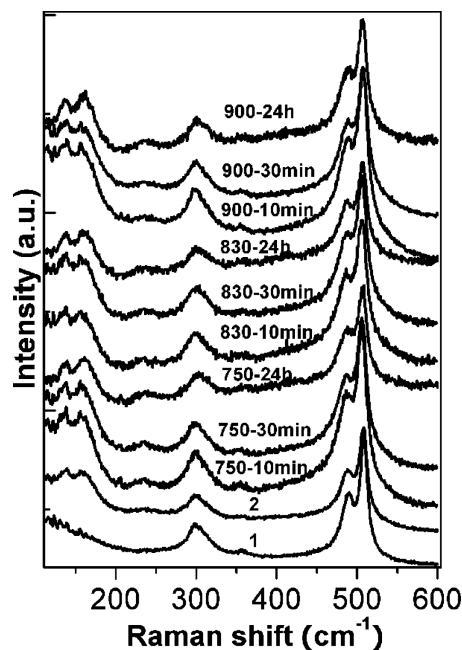


FIG. 2. Raman spectra of the samples annealed at 750°, 830°, and 900 °C. The products were denoted as x-y, where x and y represent the annealing temperature and exposure time in air, respectively. The mother zeolites (1) and Bi doped zeolites (2) annealed at 750 °C in air were used as references. Unfortunately, Raman spectra of the dehydrated samples suffer from strong fluorescence and Raman bands cannot be identified.

The structure of Y zeolite is generated by connecting sodalite units with hexagonal prisms to give a framework characterized by big, empty cavities (α -cages) with a diameter of about 13 Å and a large pore opening of 7.4 Å.¹ It is recognized that the cations are mainly located in a few well-defined sites (i.e., SI, SI', SII, SII', and SIII sites).¹⁹ Site SI is located in the center of the hexagonal prism, closely surrounded by six oxygen atoms of the two bases of the prism. Cations located in this site are almost totally inaccessible to guest molecules. Cations in site SI' are located inside the sodalite cage. These cations are accessible only to molecules able to penetrate through a six-membered ring from the supercages into the sodalite cavities. This penetration is not possible for small molecules such as CO or N₂ but occurs for H₂.^{20,21} In contrast, SII and SIII sites are accessible to CO, N₂, O₂, and H₂O molecules. Given the peculiar structural characteristics of Y zeolites and air-sensitivity of bismuth active centers in the framework, it is suggested that some Bi₅³⁺ and Bi⁺ ions locate inside of α -cages or on the surface of the zeolite, which can be destroyed by O₂ and H₂O. In view of the kept absorption band < 500 nm for the hydrated products, partial Bi₅³⁺ clusters should be inside the sodalite cage considering the space available in the hexagonal prism and the sodalite cage, which has no chance to interact with H₂O molecules owing to the existence of bismuth agglomerates (as revealed below). In the hydrated samples, most possibly, Bi⁺ mainly occupies the SI or SI' site; the absorption bands ranging from 400 to 550 nm can be attributable to Bi₅³⁺ while those at 700 and 970 nm to Bi⁺.^{18,22–24}

Since zeolites give rise to very weak Raman scattering, Raman spectra always provide an excellent method for detecting small amounts of certain inorganic ions or molecules in their structures.^{25,26} As shown in Fig. 2, Y zeolites display characteristic scattering bands in the range of 200–600 cm⁻¹, which is consistent with the results reported

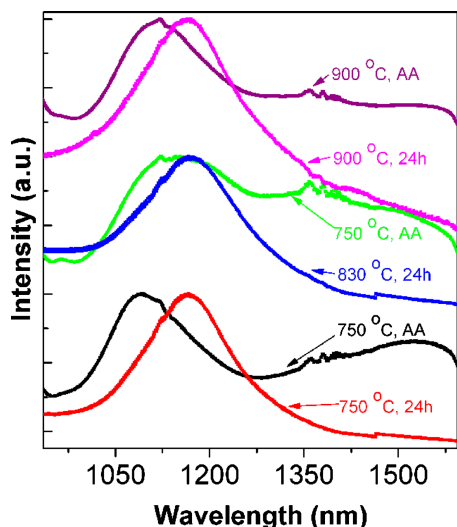


FIG. 3. (Color online) NIR PL spectra of the as-annealed (AA) and hydrated (exposure to air for 24 h) samples under 403 nm excitation. The sample annealed in air does not show NIR PL. Note that the long-wavelength (>1600 nm) signal is suppressed owing to the drop of InGaAs sensitivity.

by Dutta *et al.* and Smirnov *et al.*^{27,28} These bands can be assigned to the T–O–T bending modes (T is Si or Al). Interestingly, new bands develop at 138 and 160 cm^{-1} for Bi doped zeolites thermally treated in air and Ar atmospheres. It was reported that most cationic bismuth clusters show their characteristic scattering peaks.^{17,18,22–24} For instance, Bi_5^{3+} shows the strongest Raman scattering at $\sim 134 \text{ cm}^{-1}$. It is noteworthy that bismuth compounds can also display bands in the low-frequency range of 100–200 cm^{-1} . It was revealed by Denisov *et al.*²⁹ that Bi_2O_3 shows strong Raman scattering at ~ 138 and 150 cm^{-1} . The comparison of Raman spectra shown in Fig. 2, combined with the analysis of PL property of Bi doped zeolites, leads us to further clarify the origin of both bands at 138 and 160 cm^{-1} . The samples annealed in Ar atmosphere can show broad NIR emission (Fig. 3) while that annealed in air does not show any PL under the identical excitation condition. This phenomenon is in accordance with the results in Ref. 11, suggesting that bismuth active centers are sensitive to oxidation atmosphere and can be destroyed by oxygen. However, both NIR active and inactive zeolites doped with Bi show Raman bands at nearly identical frequencies. This indicates that the 138 and 160 cm^{-1} bands are mainly attributable to Bi_2O_3 instead of bismuth active centers such as Bi_5^{3+} . The lack of notable Raman scattering from Bi_5^{3+} in these samples might lie in their low concentration, since Bi^{3+} dominates in the samples annealed in Ar atmosphere.¹³ The above results clearly revealed that Bi_2O_3 clusters form in the zeolites, which can act as blocks for separating active centers from O_2 and H_2O .

The dehydrated zeolites show a broad emission from 930–1590 nm, consisting of a peak at ~ 1100 nm and a weak PL tail over 1250 nm; in contrast, all hydrated ones display PL bands centered at ~ 1166 nm (Fig. 3). The redshift in PL peak and the absence of long-wavelength emission tail for the hydrated samples, compared to those of dehydrated ones result from the different distribution of Bi_5^{3+} and Bi^+ active centers (i.e., the amount of Bi_5^{3+} and Bi^+ , the relative ratio of $\text{Bi}_5^{3+}/\text{Bi}^+$, and the distance between Bi_5^{3+} and Bi^+) in these samples. More detailed work is needed to further clarify the contribution of Bi_5^{3+} and Bi^+ active cen-

ters to NIR emission. This is under way in our group.

In summary, we studied Bi embedded Y zeolites through UV-vis-NIR diffuse reflectance, Raman, and steady-state NIR PL spectroscopy measurements. The results suggest that Bi_5^{3+} and Bi^+ active centers coexist in the dehydrated and hydrated zeolite framework. Furthermore, the high-temperature annealing leads to the formation of Bi_2O_3 clusters, which act as blocks for closing down the “in-out windows” of O_2 and H_2O molecules. These results present a much clearer picture on the active centers in Bi embedded Y zeolites, which may be helpful to further prepare NIR emitting zeolites containing high concentration of bismuth active centers. It is believed that these materials can find a wide array of applications as active media of broadly tunable micro or nano-optical sources.

H. Sun gratefully acknowledges the funding support from the International Center for Young Scientists and National Institute for Materials Science, Japan (Grant No. 215114).

- ¹G. L. Marra, A. N. Fitch, A. Zecchina, G. Ricchiardi, M. Salvalaggio, and S. Bordiga, *J. Phys. Chem. B* **101**, 10653 (1997).
- ²E. Borello, C. Lamberti, S. Bordiga, A. Zecchina, and C. Areán, *Appl. Phys. Lett.* **71**, 2319 (1997).
- ³S. Bordiga, G. Turnes Palomino, A. Zecchina, G. Ranghino, E. Giamello, and C. Lamberti, *J. Chem. Phys.* **112**, 3859 (2000).
- ⁴G. Calzaferri, S. Huber, H. Maas, and C. Minkowski, *Angew. Chem., Int. Ed.* **42**, 3732 (2003).
- ⁵G. Calzaferri, C. Leiggner, S. Glaus, D. Schürch, and K. Kuge, *Chem. Soc. Rev.* **32**, 29 (2003).
- ⁶M. Lezhnina and U. Kynast, *J. Alloys Compd.* **380**, 55 (2004).
- ⁷G. Calzaferri and K. Lutkouskaya, *Photochem. Photobiol. Sci.* **7**, 879 (2008).
- ⁸M. Lezhnina, F. Laeri, L. Benmouhadi, and U. Kynast, *Adv. Mater. (Weinheim, Ger.)* **18**, 280 (2006).
- ⁹D. Brühwiler, G. Calzaferri, T. Torres, J. H. Ramm, N. Gartmann, L. Dieu, I. Lopez-Duarte, and M. V. Martinez-Diaz, *J. Mater. Chem.* **19**, 8040 (2009).
- ¹⁰H. Sun, T. Hasegawa, M. Fujii, F. Shimaoka, Z. Bai, M. Mizuhata, S. Hayashi, and S. Deki, *Appl. Phys. Lett.* **94**, 141106 (2009).
- ¹¹Y. Wada, T. Okubo, M. Ryo, T. Nakazawa, Y. Hasegawa, and S. Yanagida, *J. Am. Chem. Soc.* **122**, 8583 (2000).
- ¹²K. Tanaka and A. Saitoh, *Appl. Phys. Lett.* **94**, 241905 (2009).
- ¹³H. Sun, A. Hosokawa, Y. Miwa, F. Shimaoka, M. Fujii, M. Mizuhata, S. Hayashi, and S. Deki, *Adv. Mater. (Weinheim, Ger.)* **21**, 3694 (2009).
- ¹⁴H. Sun, Y. Miwa, F. Shimaoka, M. Fujii, A. Hosokawa, M. Mizuhata, S. Hayashi, and S. Deki, *Opt. Lett.* **34**, 1219 (2009).
- ¹⁵G. Boulon, B. Moine, and J. Bourcet, *Phys. Rev. B* **22**, 1163 (1980).
- ¹⁶A. Srivastava, *J. Lumin.* **78**, 239 (1998).
- ¹⁷J. Beck and T. Hilbert, *Eur. J. Inorg. Chem.* **2004**, 2019 (2004).
- ¹⁸S. Ulvenlund, L. Bengtsson-Klo, and K. Ståhl, *J. Chem. Soc., Faraday Trans.* **91**, 4223 (1995).
- ¹⁹J. V. Smith, *Adv. Chem. Ser.* **101**, 171 (1974).
- ²⁰S. Bordiga, D. Scarano, G. Spoto, A. Zecchina, C. Lamberti, and C. Otero Areán, *Vib. Spectrosc.* **5**, 69 (1993).
- ²¹S. Bordiga, E. Garrone, C. Lamberti, A. Zecchina, C. Otero Areán, V. B. Kazansky, and L. M. Kustov, *J. Chem. Soc., Faraday Trans.* **90**, 3367 (1994).
- ²²N. J. Bjerrum, C. R. Boston, and G. P. Smith, *Inorg. Chem.* **6**, 1162 (1967).
- ²³J. Corbett, *Inorg. Chem.* **7**, 198 (1968).
- ²⁴B. Krebs, M. Mummert, and C. Brendel, *J. Less-Common Met.* **116**, 159 (1986).
- ²⁵C. Angell, *J. Phys. Chem.* **77**, 222 (1973).
- ²⁶H. Sun, M. Fujii, Y. Sakka, Z. Bai, N. Shirahata, L. Zhang, Y. Miwa, and H. Gao, *Opt. Lett.* **35**, 1743 (2010).
- ²⁷P. K. Dutta, D. C. Shieh, and M. Puri, *J. Phys. Chem.* **91**, 2332 (1987).
- ²⁸K. S. Smirnov and D. Bougeard, *J. Phys. Chem.* **97**, 9434 (1993).
- ²⁹V. N. Denisov, A. N. Ivlev, A. S. Lipin, B. N. Mavrin, and V. G. Orlov, *J. Phys.: Condens. Matter* **9**, 4967 (1997).